Tibiofemoral contact stress after total knee arthroplasty

Comparison of fixed and mobile-bearing inlay designs

Christina Stukenborg-Colsman, Sven Ostermeier, Christof Hurschler and Carl Joachim Wirth

Orthopaedic Department, Hannover Medical School, Heimchenstr. 1-7, DE-30625 Hannover, Germany. stukenborg@annastift.de
Submitted 01-07-29. Accepted 02-03-14

ABSTRACT – **We measured tibiofemoral contact stresses and the load-bearing contact area of fixed and mobile-bearing inlay knee prostheses under dynamic loading conditions. An electronic resistive pressure-measuring sensor was used to detect contact stresses and contact area in five cadaver knees. Stresses were measured with the tibial component aligned normally, as well as in internally- and externally-rotated positions. The average peak contact stresses measured on the fixed inlay were greater (medial 21 MPa and lateral 21 MPa) than those on the mobile inlay (medial/lateral 7.7/5.3 MPa, p = 0.04). Although the average peak contact stresses of the fixed standard inlay greatly exceeded the contact stresses of the other two inlay designs in each malrotated position tested, no statistically significant differences were seen. The data suggest that the ability of the inlay to translate on the tibial baseplate permits the inlay to align itself on the femoral component so that the contact surface area is maximized and contact stresses are reduced.**

Use of movable polyethylene inlays in total knee arthroplasty may permit greater conformity of the tibiofemoral joint than is possible with fixed inlay designs, thereby reducing contact stress without reducing the knee's range of motion. The decreased contact stress made possible by mobile-bearing designs is said to increase longevity of the prosthesis by reducing wear.

Several experimental approaches have been used to predict the severity and location of wear of polyethylene inserts. Finite element analysis is of value for determining changes in the stresses due to polyethylene thickness (Bartel et al. 1986, 1995, Morra et al. 1998). Contact stress analysis, using pressure-sensitive Fuji film, can provide a relatively simple, reproducible experimental technique for comparing the contact stresses of various prostheses. With this technique, several authors have reported significantly lower contact stress on the polyethylene inlay of mobile bearing designs in quasi-static studies. They recorded or calculated contact stress in sequential steps at various knee flexion angles (McNamara et al. 1994, Szivek et al. 1995, 1996).

Rotational malalignment of the tibial baseplate, which may occur during intraoperative implantation of the tibial prosthesis, has been associated with severe delamination of the polyethylene inlay (Wasielewski et al. 1994). Mobile-bearing inlays theoretically can adjust this malalignment by self-correcting movement on the tibial baseplate, which results in better wear characteristics. However, the degree of rotational correction provided by the mobile inlays is small. Current mobile-bearing inlays use guiding mechanisms such as pins and grooves to avoid subluxation of the inlay. These mechanisms may cause kinematic problems in severe cases of malalignment.

Because of the limited accuracy and repeatability of in vivo measurements, and to permit assessment of the effect of malalignment, we developed an in vitro technique to simulate isokinetic knee flexion and extension. This allows loadings that more closely approximate the magnitude of physiologic forces and moments than previously used in biome-

chanical dynamic simulations (Omori et al. 1997). Our aims were to measure tibiofemoral contact stresses and the load-bearing contact area of fixed and mobile-bearing inlay designs under dynamic loading conditions. We also evaluated tibiofemoral contact stresses in malrotated tibial tray positions for both inlay types. We tested the hypothesis that mobile-bearing inlay designs reduce contact stress more than fixed ones, especially in the presence of malrotation of the tibial baseplate.

Material and methods

The Interax system (Stryker/Howmedica/Osteonics) was implanted into the right knee of 5 fresh frozen adult cadaver knees (mean age 62 (52–75) years, 1 unknown). The knees were transected about 30 cm proximal and distal to the knee joint. The skin and subcutaneous tissues were removed, preserving the muscles, articular capsule, ligaments, and tendons. All total knee arthroplasties were done by two surgeons. The anterior cruciate ligament was removed and the posterior cruciate ligament preserved. The femoral and tibial component were aligned at zero degrees to the mechanical axis. A specially-designed implantation jig ensured correct rotational alignment. The Interax system provides a tibiofemoral articulation surface of the femoral prosthesis, which is spherically shaped in both the frontal and sagittal planes. It includes 3 types of inlay which can be used with the same femoral component: two fixed inserts, standard and high conformity (STD and HC), and one mobile meniscal-bearing (MB) insert. The knee prosthesis with the MB insert permits anterior/posterior sliding and rotation of the inlay on the tibial tray. Movement of the inlay is guided by two metal pins on the tibial tray which match the profile of a corresponding groove on the underside of the inlay. The maximum possible movement of the inlay center is 8.5 mm anterior/posterior and 18° of axial rotation relative to the tibial tray.

An electronic resistive pressure-measuring sensor (K-scan sensor: Tekscan Inc., Boston, USA) was used to assess contact stresses and contact area. The device senses the location, timing, and pressure distribution of contact stresses ranging in magnitude from 0.1–172 MPa. This is achieved by a coating material which varies in electrical resistance in proportion to the amount of pressure applied. The sensor has 2 separate sensing areas measuring 33 × 22 mm and 0.1 mm thick. The sensors consist of 26 × 22 rows and columns with intersection points that form the sensing location. Each sensing area (medial and lateral compartments) therefore comprises 572 individual sensors or "sensels". The sensors were glued to the medial and lateral compartments of the polyethylene insert so that about 95% of the inlay surface was covered. To protect the film during repeated measurements, a teflon film of 0.1 mm thickness was applied. Tibiofemoral peak contact stress and the load-bearing area were thus measured throughout the simulated motion in both the medial and lateral compartments of the prosthesis.

The K-scan sensors were preconditioned and calibrated according to the manufacturer's guidelines. These procedures were performed with the sensor in situ on the 8 mm polyethylene insert. The insert was installed on a tibial baseplate, after which the baseplate and femoral component were mounted on a servohydraulic mechanical testing system (MTS, Minneapolis, USA). The sensor was then preconditioned by repeated loading and unloading to 1500 N, and subsequently calibrated under a linearly increasing repeated load of 800–1500 N. This calibration was done before and after all measurements.

The specimens were mounted onto a specially-designed knee simulator in which isokinetic flexion-extension motions are simulated (Figure 1). The knee specimens were oriented with the femur fixed horizontally and the patella facing downwards. The tibia was attached to the simulator at mid-length by means of a linear-rotational bearing which permits axial sliding and turning, as well as rotation transverse to the axis of the tibia. The bearing in turn was attached to a swing-arm which allows varus-valgus rotation. The resulting arrangement gives complete freedom of motion of the joint, with the exception of flexion-extension, which is determined by the position of the swing-arm. The swing-arm was equipped with a strain-gage based load-measuring device which allows the torsional moment applied to the tibia to be monitored continuously.

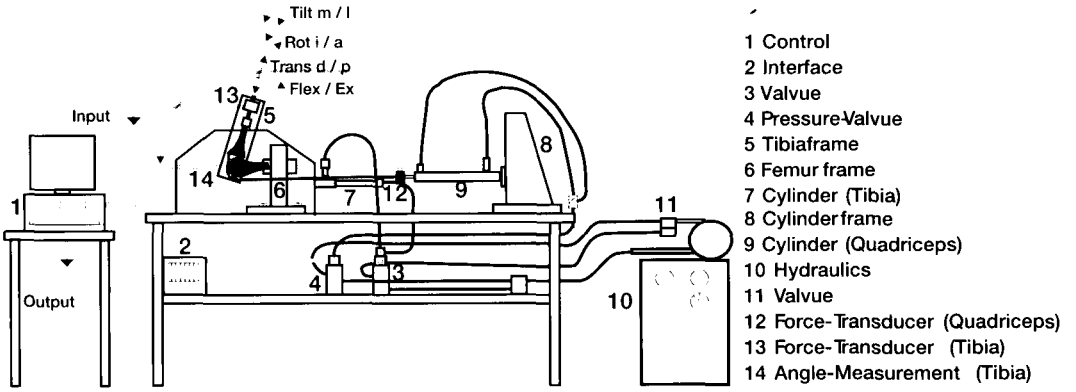

Figure 1. Knee simulator.

Movement of the tibia was generated by the coordinated activation of two hydraulic cylinders, one to simulate quadriceps muscle force, and the other to apply an external flexion moment. A specially-constructed tendon clamp, which allowed application of loads up to 2000 N, was used to attach the quadriceps tendon to the hydraulic cylinder with a steel cable. Quadriceps force was measured with a load cell attached to the quadriceps cylinder. The external flexion moment was applied to the specimen by the second hydraulic cylinder by means of a rack-and-pinion mechanism attached to the swing-arm. The flexion cylinder was calibrated to provide a flexion rotational moment of 31 Nm or 39 Nm.

The experiments were done using the following protocol: first, the swing-arm was activated to bring the specimen into a position of 120° of flexion, determined by a mechanical limiting device; the quadriceps cylinder was then activated in feedback-control to provide a constant net joint moment nominally greater than that resisted by the swing-arm. The joint moment was measured directly by the load-cell in the swing-arm. Thus, starting at 120° flexion of the knee, quadriceps force was continuously controlled to maintain the nominal extension moment during extension from 120° to 0° of flexion. The test mimicked both the speed and resulting moment of a lower limb isokinetic extension test, generating an extension torque of 31 Nm or 39 Nm, respectively.

Tibial inlay pressure distribution was measured continuously throughout the isokinetic extension motion. To study the effect of tibial baseplate malalignment, the experiments were performed with the tibial baseplate aligned normally, as well as in internally- and externally-rotated positions. The tibial baseplate was first implanted in neutral rotation and the tests performed. By means of a specially-designed implantation jig, rotational malalignment relative to the femoral component was simulated and the tests were repeated after sequential internal and external rotation of the baseplate of 5°, 10°, and 15°, respectively, relative to the tibia.

The experiment protocol was as follows: the standard STD inlay was first implanted and tested, followed by the highly conformed and the mobile-bearing inlays. Each inlay was first tested in neutral rotation, after which the tibial base-plate was rotated sequetially to each of the malrotation positions. We measured the mean maximum peak contact stress for each inlay type, and compared the medial and lateral compartment peak contact stresses.

Statistics

A multifactorial ANOVA was done to study the statistical significance (factors: inlay, side, rotation, and alignment). Statistical post hoc comparisons were done, using the nonparametric Wilcoxon signed-rank test at a significance level of $\alpha = 0.05$ (Snedecor and Cochran 1989). Results are reported with standard deviations (SD).

Results

The maximum quadriceps muscle forces exerted during extension averaged 1250 (100) N at about

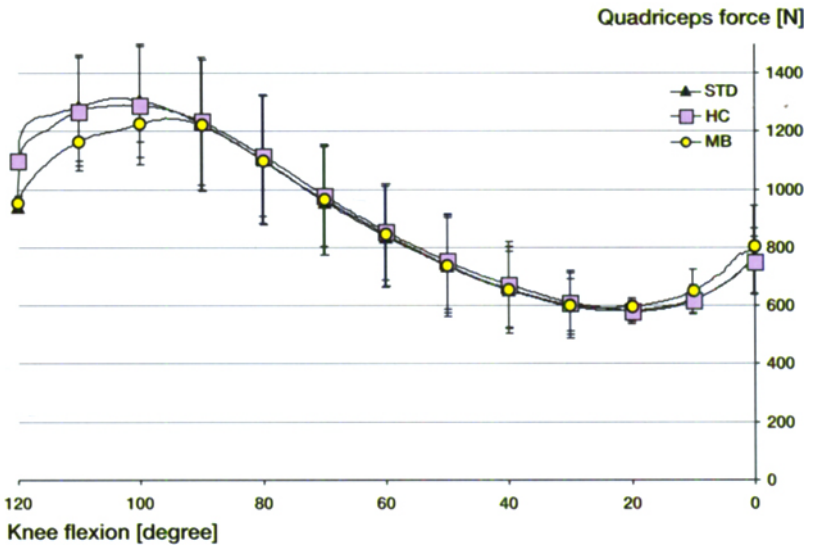

Figure 2. Quadricpes extension force at 31 Nm extension moment with SD.

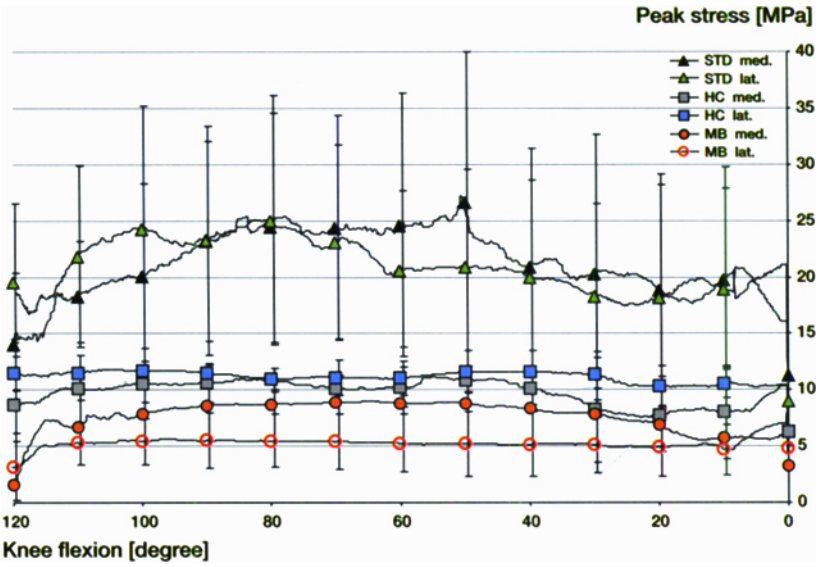

Figure 3. Peak contact stresses for the medial and lateral compartments (fixed standard (STD), high-conformity (HC), and mobile-bearing (MB) inlays (at 31 Nm extension moment, SD)

100° of knee flexion. The extension moment measured was held nearly constant during the motion. The minimum force recorded during the motion was 600 (10) N at 20° of flexion (Figure 2).

Neutral position–fixed standard inlay

Contact stress through the range of the knee flexion angle varied most for the standard inlay. Thus, the maximum peak contact stress occurred in the medial compartment of the standard inlay which showed 27 (14) MPa at 31 Nm of extension moment at 50° of flexion (Figure 3; Table). At angles greater than and less than this flexion angle, peak contact stresses decreased to a minimum of

Peak contact stresses (MPa) for the medial and lateral compartments (fixed standard, high-conformity, and mobile-meniscal inlays)

Extension moment		Flexion degrees	Stress med.	SD	Flexion degrees	Stress lat.	SD
Fixed standard inlay (STD)							
31 Nm	Max	51	27	14	78	25	12
	Min	0	11	14	0	8.9	12
39 Nm	Max	84	33	21	69	36	24
	Min	0	5.6	9.7	0	5.1	8.9
Fixed high-conformity inlay (HC)							
31 Nm	Max	55	11	1.2	105	12	1.0
	Min	0	6.3	1.2	0	6.2	1.0
39 Nm	Max	87	12	1.2	36	13	2.2
	Min	0	6.0	6.9	0	6.2	7.2
Meniscal-bearing inlay (MB)							
31 Nm	Max	64	8.9	3.1	0.2	8.3	2.8
	Min	120	1.5	3.1	120	3.1	2.8
39 M	Max	118	11	10	1.0	8.3	4.3
	Min	0	3.5	4.2	120	4.4	3.5

8.5 (12) MPa. The average peak contact stresses for the entire extension cycle were 21 (0.1) MPa in the medial and 21 (0.1) in the lateral compartment (31 Nm). At an extension moment of 39 Nm, the average peak contact stresses increased to 27 (0.2) in the medial and 30 (0.2) in the lateral compartment, while showing the same characteristic form throughout the extension cycle as at 31 Nm. The maximum peak contact stress that occurred was 36 (24) MPa (39 Nm) (Table). Overall, the average peak contact stresses in the medial compartment were higher than those in the lateral compartment throughout the extension cycle.

Neutral position–fixed high-conformity inlay

The average peak contact stresses throughout the extension cycle for the fixed high-conformity inlay were 9.8 (2.1) MPa (medial) and 11 (1.5) MPa (lateral) at 31 Nm of extension moment. Average peak contact stresses at 39 Nm were 11 (2.4) MPa (medial) and 13 (1.7) MPa (lateral). The maximum peak contact stresses were 11 (1.2) MPa in the medial compartment, and 12 (1.0) MPa in the lateral compartment at 31 Nm extension moment (12 (1.2) MPa, and 13 (2.2) MPa, respectively, at 39 Nm). The lowest contact stresses were measured between the flexion angles of 0° to 40°. We found no significant differences between the medial and lateral compartment pressures for the fixed HC inlay (Figure 3; Table).

Neutral position–mobile-bearing inlay

The peak contact stresses of the 5 specimens averaged over the entire extension cycle for the mobile bearing inlay were 7.7 (2.8) MPa in the medial, and 5.3 (2.5) MPa in the lateral compartment at an extension moment of 31 Nm (9.3 (5.1) MPa, and 6.4 (2.8) MPa, respectively, at 39 Nm). The maximum peak contact stresses were 8.9 (3.1) MPa medially, and 8.3 (2.8) MPa laterally during an extension moment of 31 Nm (11 (10) MPa, and 8.3 (4.3) MPa, respectively, at 39 Nm) (Figure 3; Table).

The maximum peak contact stresses and the average contact stresses over the entire extension cycle of the fixed standard inlay were significantly greater than those of the fixed high-conformity (medial/lateral, $p = 0.04/0.04$; 31 Nm extension moment) and the mobile bearing (medial/lateral inlays, $p = 0.04/0.04$; 31 Nm). No differences were detected between the fixed high-conformity and the mobile-bearing inlays (medial/lateral, $p = 0.8/0.1$) (Figure 3).

Malrotated positions–all designs

Maximum peak contact stresses measured during tibial baseplate internal or external malrotation of 5°, 10°, or 15° varied greatly for all 3 inlay components tested. The average peak contact stresses of the fixed STD inlay tended to exceed greatly the contact stresses of the other 2 inlay designs

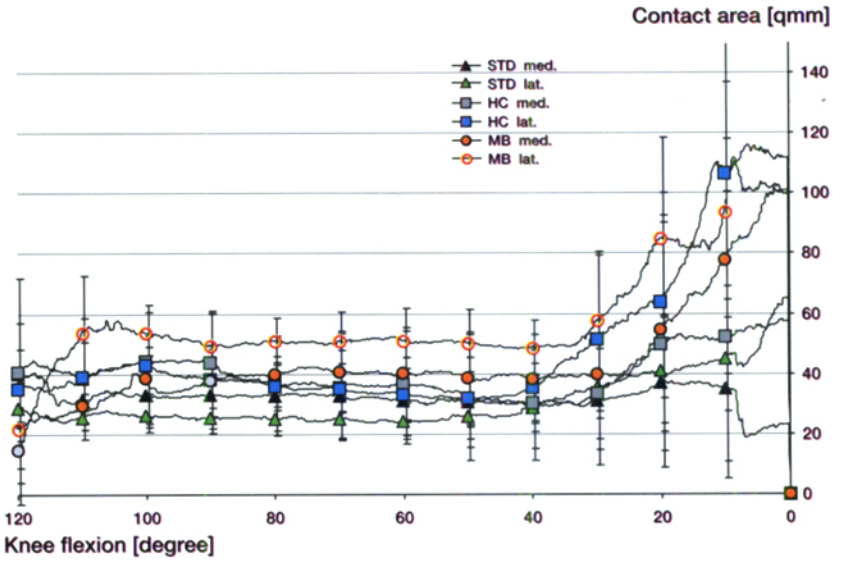

Figure 4. Contact areas for fixed and mobile-bearing inlays at 31 Nm with SD

in each malrotated position tested, although the data varied very much. Statistical analysis showed values ranging from $p = 0.06$ to $p = 0.7$ (Wilcoxon signed rank test, $\alpha = 0.05$).

Contact area in neutral position–all designs

The average maximum contact areas under 31 Nm of extension moment were found to be 119 (42) mm^2 for the fixed standard inlay, 174 (36) mm^2 for the high-conformity inlay, and 215 (39) mm^2 for the mobile-bearing inlay. The contact areas of the high-conformity and mobile-bearing inlays were significantly larger ($p = 0.04$; 31 Nm) (Figure 4). The initial starting point of the location of contact varied greatly between specimens. However, each inlay design moved in a characteristic way throughout the extension cycle. The contact areas of both the standard and fixed high-conformity inlays were located at the posterior aspect of the inlay at 120° flexion. During extension motion to 100° flexion, this contact area moved slightly forward. From 100° flexion to full extension, the contact area again moved backwards to the posterior edge of the inlay. Overall, the movement of the contact area in the lateral compartment was greater than that in the medial compartment. In contrast, the mobile-bearing inlay showed a more central and larger contact area. The contact area remained at about the center of the inlay during the entire extension cycle, which reduces the risk of edge loading.

Discussion

Tibiofemoral contact areas and contact pressure are of great interest in the native as well and prosthetic knee (Bartel et al. 1986, Collier et al. 1991, McNamara et al. 1994, Bartel et al. 1995, Szivek et al. 1995, 1996, Takahashi et al. 1997). Excessive intraarticular pressure has been recognized as an important factor in the etiology of osteoarthrosis as well as the wear and fatigue failure of polyethylene after total knee arthroplasty (Harris et al. 1999). Examinations of retrieved tibial inserts have shown that designs with low conformity and thickness of the polyethylene insert, which cause higher contact stresses, are associated with increased wear (Collier et al. 1991, Wright et al. 1992). Several authors have therefore recommended a minimal thickness of 8 mm of the tibial inserts (Bartel et al. 1986, 1995). To deal with this problem, recent knee prosthesis designs have incorporated movable polyethylene inlays. These systems permit higher conformity of the tibiofemoral joint, which reduces contact stress, without simultaneously reducing the range of motion (Buechel and Pappas 1989, Polyzoides et al. 1996). In this study, we found that

tibiofemoral contact stresses were reduced by 66% with a mobile-bearing design as compared to the standard prosthesis design. Furthermore, while the standard design showed large, variable increases in peak contact stress due to rotational malalignment, no such increases were seen with the mobile-bearing one.

The reliability of the electronic resistive pressure-measuring sensor (K-scan sensor, Tekscan Inc., Boston, USA) was verified in studies by Harris et al. (1999) and Matsuda et al. (1995, 1998) in which the sensor measurement was compared to the contact area measurements, obtained using Fuji pressure-sensitive film (Fuji Photo Film Co., Tokyo, Japan). Matsuda et al. (1995) showed that both the films and the sensor accurately measured the contact area under high load, but that the K-scan sensor measured the contact area more accurately than the Fuji film under low load. The peak stress measured with the K-scan sensor increased gradually as the load increased, but with the Fuji film, the peak stresses did not increase beyond 980 N (Matsuda et al. 1998). Harris et al. (1999) found that the contact area measured with the Fuji films was 11–36% lower than those measured with the K-scan sensor. Szivek et al. (1995) also reported that at lower load levels (667 N) Fuji film underestimated contact area, while displaying a speckled appearance related to the polyethylene surface roughness. The major advantage of the K-scan system in this study was the ability to record data continuously "real-time" during dynamic flexion/extension motions of the joint. The results can be shown in two or three dimensions, and false pressure "spikes", caused, for instance, by sensor crimping, can be filtered out of the display and the final data (Harris et al. 1999). The sensor can be sterilized and thus used in vivo during surgical procedures (Matsuda et al. 1998, Wallace et al. 1998). One inherent disadvantage of the K-scan system, common to other pressure-measuring systems using foils or membranes, is its finite thickness. The thickness of the sensor, although only 0.1 mm, may alter the contact area and pressure levels attained since the topography of the bearing surface has been changed slightly (Ateshian et al. 1994, Harris et al. 1999). Nevertheless, although some bias may exist due to the presence of the sensor, we assume that the effect of this bias is negligible in comparative studies such as this.

In a finite element study, Bartel et al. (1995) suggested that designs with more conforming articulating surfaces and thicker polyethylene inserts have an advantage. The various knee designs modeled were all predicted to produce contact stresses of ≤ 60 MPa in flexion under a load of 3000 N. The contact pressure computed by Morra et al. (1998) in another three-dimensional finite element model (full extension, 1950 N load) was similar to the pressure experimentally measured in our study for the Interax mobile-bearing inlay, although the contact area computed at 553 mm^2 was much larger than that experimentally measured (140 mm^2).

In vitro tibiofemoral contact area and pressure distributions of various knee prosthetic designs have been widely reported. Most of these studies have used Fuji film to measure contact stresses in various implant designs (Collier et al. 1991, McNamara et al. 1994, Szivek et al. 1995, 1996). Szivek et al. (1995) used Fuji films that were sensitive to pressures of 9.8–49 MN/m^2 (MPa). Knees were tested at loads of 667 N and 2000 N at 0°, 15°, and 60° of flexion for 6 TKA systems. Each test series was carried out at: 24 °C, to permit comparison with published results; at 37 °C, to allow evaluation of stresses at physiologic conditions; and at 55 °C, to assess the temperature sensitivity of stresses for each implant. At 24 °C, contact stresses were found to range between 12–28 MPa, and at 37 °C, between 13–25 MPa. Contact stresses for all components decreased as temperature increased. In general, the lowest stresses occurred at 15° flexion and increased with increasing flexion angle. In a second study, Szivek et al. (1996) included a prosthetic design with a movable meniscal inlay (LCS, DePuy, Warsaw, USA) and found that this design had the largest overall contact area, with a big area of contact in the lowest stress range (< 10 MPa). However, the testing also showed that all designs had some contact areas where maximum stresses in excess of 15 MPa (range 10 MPa–20 MPa) were recorded. The peak contact stresses ranged from ≤ 15 MPa at 15° flexion, to as high as ≥ 30 MPa at 60° flexion. Since the yield strength of UMWPE is about 15 MPa, all tibial inserts could yield to some extent.

McNamara et al. (1994) showed a small reduction in contact stress resulting from creep and wear. The contact stress for nonconforming designs also remained well above those for the more conforming devices. The contact pressure for the meniscal-bearing LCS (11–22 MPa) prosthesis and the designs with fixed bearings are comparable to the peak contact stresses measured by Szivek et al. (1996), although both Szivek and McNamara recorded or calculated the contact area and pressure in sequential steps of different knee flexion angles under static conditions. In the present study, peak contact stresses on the fixed (STD) inserts were found to be as high as 27 MPa at flexion angles of 50°, decreasing with increasing extension. The HC and MB inlays, however, showed average peak contact stresses of only 12 MPa and 9 MPa, respectively, a significant reduction. Thus, in our study and in those of the literature, significantly lower contact stresses and larger contact areas were measured with the mobile inlay prosthetic designs.

Matsuda et al. (1998), using the K-scan sensor under static conditions, found increasing peak contact stresses with increasing flexion angles using both fixed and movable inlay designs (range 15 MPa–40 MPa). In addition, they showed that internal and external rotational malalignments of 15° of the tibial baseplate increased surface stresses significantly with the fixed inserts. Mobile-bearing inlays could mitigate this effect significantly with increasing rotation of the insert. Arizono et al. (1999), however, found no significant differences in peak pressure with a malrotated tibial component. In the present study, large, but very variable, increases in contact stresses with rotational malalignment were seen with the standard design, while these increases were not observed with the high-conformity and mobile-bearing designs.

Our data suggest that the ability of the inlay to translate on the tibial baseplate permits the inlay to align itself on the femoral component so that contact is maximized and contact stresses are reduced. This feature of mobile-bearing inlays reduces the likelihood of cold flow and stress-peak damage.

We thank the Stryker/Howmedica/Osteonics Company for their financial support of this study.

Arizono T, Emoto G, Whiteside L A. Effect of malrotation on tibiofemoral articular contact pressure and kinematics with a conforming tibial articulation in total knee replacement. 45th Annual Meeting, Orthopaedic Research Society, February 1-4, 1999, Anaheim, California. 1999.

Ateshian G, Kwak S, Soslowsky L, Mow V. A stereophotogrammetric method for determining in situ contact areas in diarthrodial joints, and a comparison with other methods. J Biomech 1994; 27: 111-24.

Bartel D L, Bicknell V L, Wright T M. The effect of conformity, thickness, and material on stresses in ultra-high molecular weight components for total joint replacement. J Bone Joint Surg (Am) 1986; 68: 1041-51.

Bartel D L, Rawlinson J J, Burstein A H, Ranawat C S, Flynn W F Jr. Stresses in polyethylene components of contemporary total knee replacements. Clin Orthop 1995; 317: 76-82.

Buechel F F, Pappas M J. New Jersey low contact stress knee replacement system. Ten-year evaluation of meniscal bearings (published erratum appears in Orthop Clin North Am 1989; Oct 20 (4): preceding 519). Orthop Clin North Am 1989; 20: 147-77.

Collier J P, Mayor M B, McNamara J L. Analysis of the failure of 122 polyethylene inserts from uncemented tibial knee components. Clin Orthop 1991; 273: 232-42.

Harris M L, Morberg P, Bruce W J M, Walsh W R. An improved method for measuring tibiofemoral contact areas in total knee arthroplasty: a comparison of K-scan sensor and Fuji film. J Biomech 1999; 32: 951-8.

Matsuda S, Williams V G, Whiteside L A, White S E. A comparison of pressure-sensitive film and digital electronic sensors to measure contact area and contact stress. 41st Annual Meeting, Orthopaedic Research Society, February 13-16, Orlando, 1995: 743.

Matsuda S, White S E, Williams V G, McCarthy D S, Whiteside L A. Contact stress analysis in meniscal bearing total knee arthroplasty. J Arthroplasty 1998; 13: 699-706.

McNamara J L, Collier J P, Mayor M B, Jensen R E. A comparison of contact pressures in tibial and patellar total knee components before and after service in vivo. Clin Orthop 1994; 299: 104-13.

Morra E A, Postak P D, Greenwald A S. The influence of mobile bearing knee geometry on the wear of UHMWPE tibial inserts: A finite element study. 1. 1998. Ohio, Orthopaedic Research Laboratories.

Omori G, Koga Y, Bechthold J E, Gustilo R B, Nakabe N, Sasagawa K, Hara T, Takahashi H E. Contact pressure and three-dimensional tracking of unresurfaced patella in total knee arthroplasty. The Knee 1997; 4: 15-21.

Polyzoides A J, Dendrinos G K, Tsakonas H. The Rotaglide total knee arthroplasty. Prosthesis design and early results. J Arthroplasty 1996; 11: 453-9.

Snedecor G W, Cochran W G. Statistical methods. Iowa State University Press, Ames, Iowa, 1989.

Szivek J A, Cutignola L, Volz R G. Tibiofemoral contact stress and stress distribution evaluation of total knee arthroplasties. J Arthroplasty 1995; 10: 480-91.

Szivek J A, Anderson P L, Benjamin J B. Average and peak contact stress distribution evaluation of total knee arthroplasties. J Arthroplasty 1996; 11: 952-63.

Takahashi T, Wada Y, Yamamoto H. Soft-tissue-balancing with pressure distribution during total knee arthroplasty. J Bone Joint Surg (Br) 1997; 79: 235-9.

Wallace A, Harris M, Walsh W, Bruce W. Intraoperative assessment of tibiofemoral contact stresses in total knee arthroplasty. J Arthroplasty 1998; 13: 923-7.

Wasielewski R C, Galante J O, Leighty R M, Natarajan R N, Rosenberg A G. Wear patterns on retrieved polyethylene tibial inserts and their relationship to technical considerations during total knee arthroplasty. Clin Orthop 1994; 299: 31-43.

Wright T M, Rimnac C M, Stulberg S D, Mintz L, Tsao A K, Klein R W, McCrae C. Wear of polyethylene in total joint replacements. Observations from retrieved PCA knee implants. Clin Orthop 1992; 276: 126-34.